Materials Science & Engineering A 620 (2015) 454–462

Contents lists available at ScienceDirect

Materials Science & Engineering A

journal homepage: www.elsevier.com/locate/msea

Structure–mechanical property relationship in a low carbon Nb–Cu microalloyed steel processed through a three-step heat treatment: The effect of tempering process

W.H. Zhou [a], V.S.A. Challa [b], H. Guo [a], C.J. Shang [a,*], R.D.K. Misra [b]

[a] School of Materials Science and Engineering, University of Science and Technology, Beijing, China
[b] Department of Metallurgical and Materials Engineering, University of Texas El Paso, TX 799968, USA

ARTICLE INFO

Article history:
Received 27 August 2014
Received in revised form
16 September 2014
Accepted 19 September 2014
Available online 28 September 2014

Keywords:
Microalloyed steel
Tempering
Retained austenite
Mechanical properties
Precipitates

ABSTRACT

We describe here the impact of tempering temperature and tempering time on the microstructure and mechanical property in a low carbon Nb–Cu microalloyed steel via a three-step heat treatment. After tempering process, the microstructure primarily comprised of ferrite, retained austenite and tempered bainite/martensite. The ferrite matrix with ultrafine grain size was film-like and enriched with nanometer-sized niobium-containing and copper precipitates. The volume fraction of ferrite increased with the increase in tempering temperature and tempering time. Retained austenite had average grain size less than 1 μm and was enriched with copper precipitates that contributes to enhance the stability of austenite. The retained austenite revealed high thermal stability and remained stable in the range of 20–30% when tempering temperature and time changed. High strength and good ductility were obtained in the tempering temperature range of 450–550 °C, or by prolonging tempering time at 500 °C, where the yield strength was ~750 MPa and the product of tensile strength and % elongation was ~32 GPa%, which is attributed to the cooperation of multiphase microstructure, stable retained austenite and nanometer-sized precipitates.

1. Introduction

It is well known that retained austenite plays a great role in a multiphase system to obtain high strength and excellent ductility in steel. One promising and innovative heat treatments for the creation of retained austenite is annealing reverted transformation process (ART) [1–4]. In this process, retained austenite was obtained by the stabilization of reverted austenite through the diffusion of Mn or Ni from nearby martensite during the intercritical annealing process in high Mn/Ni martensitic steels.

On the basis of ART process, a two-step intercritical heat treatment was proposed by present authors to produce retained austenite in a low carbon Cu-bearing and Nb-microalloyed steel [5,6]. Retained austenite with volume fraction more than 20% was obtained by successive enrichment of Mn and Ni in the reversed austenite during each intercritical process. Because of high intercritical temperature, the precipitation was inadequate, such that precipitation strengthening effect was minimal. Thus, it is essential to introduce a third tempering step to make full use of precipitation of niobium and copper.

However, the tempering process generally leads to the decomposition of retained austenite into ferrite and cementite, which is detrimental to the ductility. In previous work from Thomas [7], the decomposition temperature of retained austenite increased with increase in concentration of Mn and Ni in a medium carbon steel, which means that the thermal stability of retained austenite can be enhanced by the enrichment of Mn and Ni. It is possible for the retained austenite obtained by two-step heat treatment to remain stable during tempering process. Nevertheless, there is still a lack of experimental evidence to document the behavior of retained austenite in tempering process.

From the above discussions, the third tempering process has a great impact on both the precipitation behavior and retained austenite content. Since the combination of retained austenite and precipitates is widely applied to develop advanced high strength steel (AHSS) [8,9], it is necessary and significative to make clear the relationship between the tempering process parameters and the microstructural features and the relative mechanical properties. In this regarding, present work is to study the effect of tempering temperature and time on the microstructure–mechanical property

* Corresponding author. Tel.: +86 10 62322428; fax: +86 10 62332428.
E-mail address: cjshang@ustb.edu.cn (C.J. Shang).

http://dx.doi.org/10.1016/j.msea.2014.09.079
0921-5093/

relationship in a Nb–Cu microalloyed steel to explore the potential of the studied steel.

2. Experimental procedures

The nominal chemical composition of experimental steel in wt % was Fe–0.10C–2.01Mn–0.78Si–0.78Al–0.08Nb–1.01Cu–1.0Ni–0.26Mo. The role of different alloying elements is discussed elsewhere [5]. The optimal temperatures for the two-step heat treatment were confirmed to be 780 °C and 660 °C [6], which remained same in the three-step process described in the present study. To study the influence of third-step tempering process on the microstructure and mechanical properties, the tempering temperature was varied from 400 to 640 °C with tempering time of 30 min. Similarly, to study the tempering time, the tempering temperature was kept constant at 500 °C and the tempering time was changed from 30 to 120 min (Fig. 1).

Heat treated samples were mounted and mechanically polished to mirror finish using standard metallographic procedures. The specimens were etched with 2% nital for optical and scanning electron microscopy (SEM) observation. SEM was performed using ZEISS ULTRA-55 field emission scanning electron microscopy in conjunction with electron back scatter diffraction (EBSD) operated at 20 kV. The EBSD scans were carried out at a step size of 0.8 μm. The ferrite, retained austenite and bainite/martensite was clearly differentiated by mixed etchant of picric and $Na_2S_2O_5$ [10]. With this technique, ferrite appears tan or light yellow, bainite is brown, and retained austenite and martensite are both white. Retained austenite was quantified by X-ray diffraction (XRD) using CuKα radiation and the volume fraction estimated by measuring the peak intensity of (200)α, (211)α, (200)γ, (211)γ and (311)γ. The volume fraction of ferrite was estimated by an automatic counting technique using an image analyzer.

Hardness measurement was conducted in a Vicker's hardness tester under 1 kg applied load and the average hardness of a particular sample was reported from measurement over 10 locations. Tensile properties were measured at room temperature using standard tensile samples machined to 5 mm diameter and 25 mm gauge length according to ASTM E8 specification. To characterize the fine-scale microstructure, transmission electron microscopy (TEM) was carried out using 3 mm disks that were twin-jet electro-polished in an electrolyte of 10% perchloric acid and 90% ethanol. TEM was carried out using a Hitachi H7600 and JEOL JEM-2100 FS microscope equipped with an energy dispersive X-ray spectrometer (EDS) operated at 120 kV and 200 kV, respectively.

3. Experimental results

3.1. Mechanical properties

Yield strength (YS), tensile strength (TS), uniform (UEL) and total (TEL) % elongation as a function of tempering temperature are presented in Fig. 2. In the three-step heat treatment, when the tempering temperature was increased from 400 °C to 640 °C, the yield strength was in the range of 681–756 MPa, tensile strength was 839–952 MPa, uniform elongation was 18–23%, and total elongation was 28–38% (Fig. 2a). The best combination of strength and ductility was obtained at 500 °C and 550 °C, when the yield strength was greater than 720 MPa and the total elongation was ~30%. With increase in tempering temperature, the tensile strength was decreased, whereas the yield strength was similar (Fig. 2b). Even though the tempering temperature varied over a large range, the uniform and total elongation were high. This means that the tempering temperature had little impact on the ductility of the studied steel. In comparison to the two-step process, the three-step treatment significantly enhanced the strength, especially the tensile strength without losing ductility.

On tempering at 500 °C, when the tempering time was increased from 30 min to 120 min, the yield strength increased from 724 MPa to 756 MPa, total elongation increased from ~30% to ~37%, and uniform elongation remained stable at ~22% with a small loss in tensile strength (Table 1). This suggests that the mechanical properties can be further enhanced by prolonging the tempering time.

3.2. Microstructure characterization

Fig. 3a is optical micrograph of three-step heat-treated steel sample at tempering temperature of 500 °C after Lepera etching. The areas with light yellow color refer to ferrite, the brown color reveals the lath of bainite, and the white color is martensite and retained austenite. Given the sample underwent a successive tempering process, the martensite content was low. In the light of the distribution, size and morphology of retained austenite that were characterized by EBSD in Fig. 3b, it can be concluded that the white area with small size in Fig. 3a is retained austenite. This also

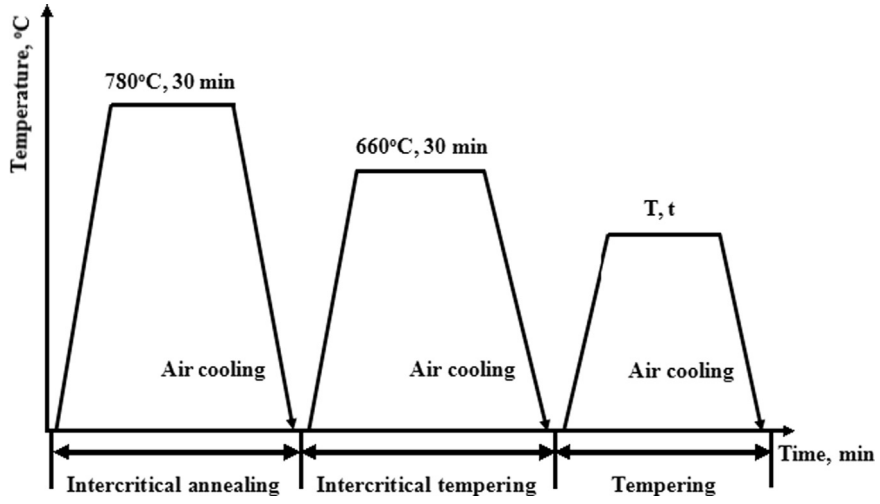

Fig. 1. Schematic diagram of three-step heat treatment. (i) The tempering temperature *T* varies in the range of 400–640 °C at a constant tempering time (*t*) of 30 min. (ii) The tempering time *t* changes from 30 min to 120 min at a constant tempering temperature of 500 °C.

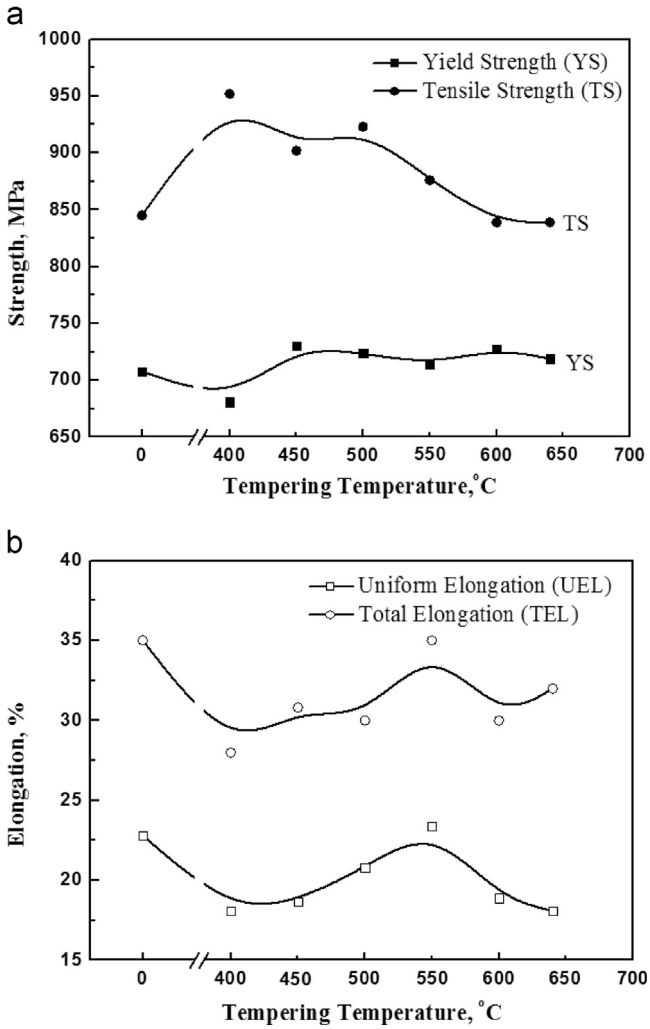

Fig. 2. (a) Yield and tensile strength and (b) uniform and total elongation as a function of tempering temperature in the experimental steel processed by three-step heat treatment.

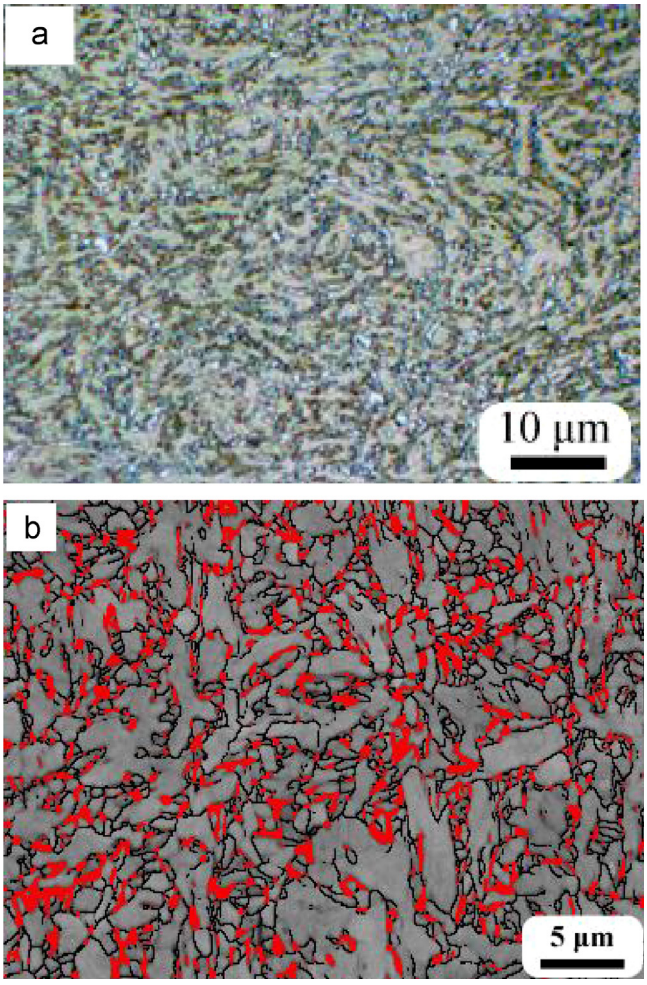

Fig. 3. Light (a) and EBSD (b) characterization showing the distribution of retained austenite in the microstructure of experimental steel after three-step heat treatment at tempering temperature of 500 °C. (b) The red areas represent retained austenite and the black lines in (b) denote grain boundaries with misorientation $\geq 5^{\circ}$. (For interpretation of the references to color in this figure legend, the reader is referred to the web version of this article.)

Table 1
The mechanical properties of investigated steel tempered at 500 °C for different time in three-step heat treatment.

Time, min	YS, MPa	TS, MPa	UEL, %	TEL, %
30	724 ± 3	923 ± 5	20.8 ± 0.4	29.8 ± 1
60	752 ± 3	851 ± 2	22.6 ± 1	37.8 ± 2
120	756 ± 5	895 ± 4	22.3 ± 1	36.6 ± 2

provides evidence for the recognition of retained austenite and bainite/martensite in the following SEM micrographs.

Representative scanning electron micrographs (SEM) of experimental steel tempered at different tempering temperatures are presented in Fig. 4. The microstructure comprised of ferrite, retained austenite, and tempered bainite/martensite. There was no obvious change in the microstructure of the steel tempered at 500 °C for different times (Fig. 5). The ferrite matrix had ultrafine grain size and was surrounded by bainite/martensite and retained austenite. Similar nature of ferrite was observed in Q-P steel and medium manganese-containing steel [11].

Two types of retained austenite were observed by TEM observation: film-like that was present between bainitic/martensitic laths (Fig. 6), and the blocky that was present at ferrite/ferrite or ferrite/bainite or martensite boundaries (Fig. 7). The selected area diffraction (SAD) pattern confirmed the orientation relationship between retained austenite and ferrite was [100]α//[110]γ, implying a N–W relationship [12]. The difference in morphology is related to the initial microstructure, where retained austenite nucleates and grows. The ferrite was film-like, and only a small amount of ferrite was quasi-polygonal at low tempering temperature. On tempering at high temperatures, the quasi-polygonal ferrite was the dominant microstructure. These ferrite grains were in size range of 1–2 μm and their boundaries were visible. This transition in the morphology of ferrite from film-like to quasi-polygonal indicates that new ferrite was formed when the temperature was greater than 600 °C.

The TTT plot of nominal chemical composition predicts that the microstructure at 600 °C primarily consists of ferrite and pearlite (Fig. 8). The pearlite can only be obtained at cooling rate of ~0.1 °C/s. Moreover, pearlite was not observed in the first two steps [6], where the temperature was high. For this reason, the pearlite transformation can be neglected here. On the other hand, the enrichment of alloying elements in the reversed austenite during two-step process significantly decreases A_1 temperature, which means that the ferrite transformation starts at a lower temperature in the alloy-enriched austenite. Therefore, ferrite

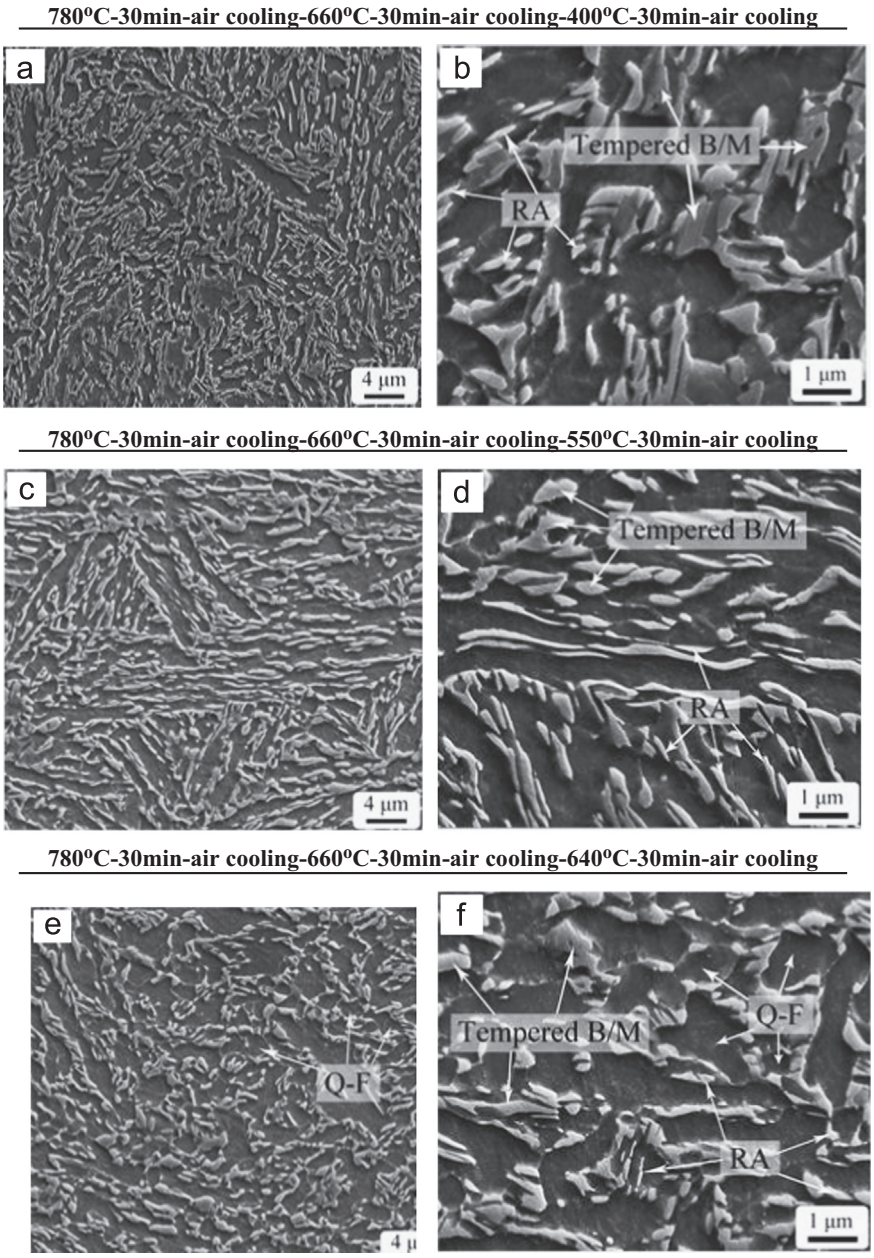

Fig. 4. Low and high magnification SEM micrographs of samples tempered at different tempering temperatures (a, b) 400 °C; (c, d) 550 °C; (e, f) 660 °C after two-step intercritical annealing and intercritical tempering treatment. RA: retained asutenite, B/M: bainite or martensite, and Q-F: quasi-polygonal ferrite.

transformation probably occurs in austenite at high tempering temperature, resulting in increase of volume fraction of ferrite at high temperature (Fig. 9a).

The dominant microstructure of experimental steel tempered at 500 °C for different times was film-like ferrite lath and retained austenite. The quantitative analysis revealed that the volume fraction of ferrite increased with increase in tempering time (Fig. 9b). This might be caused by the recovery of bainite/martensite that can be referred as ferrite since most of manganese and carbon atoms in bainite/martensite has escaped into austenite or formed precipitates after the tempering process.

3.3. The behavior of retained austenite during the tempering process

The volume fraction of retained austenite as a function of tempering temperature and tempering time are presented in Fig. 9. With increase in tempering temperature from 400 °C to 600 °C, the volume fraction of retained austenite remained stable over the range of 20–30% (Fig. 9a). When the tempering time was increased from 30 min to 120 °min at a constant tempering temperature of 500 °C, the volume fraction of retained austenite was decreased from ~30% to ~20% (Fig. 9b). Despite the tempering temperature and time vary over a large range, high volume fraction of retained austenite greater than 20% can be obtained. The volume fraction of retained austenite obtained through intercritical heat treatment is determined by the competition between reversed austenite content and the enrichment of alloying elements. However, the reversion transformation was not responsible for the change in retained austenite content in the tempering process. First, the diffusion of alloying elements can be neglected during the tempering process because of low temperature, such that the enrichment of alloying elements hardly occurs. Second,

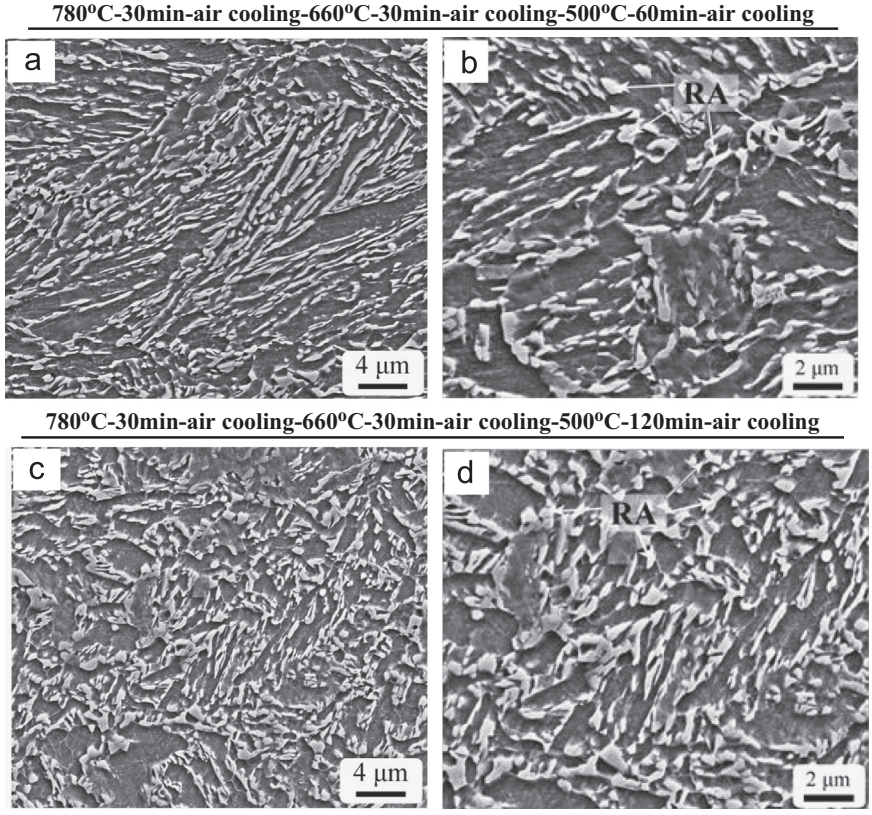

Fig. 5. Low and high magnification SEM micrographs of samples tempered at different tempering time (a, b) 60 min; (c, d) 120 min at constant tempering temperature of 500 °C in the three-step heat treatment.

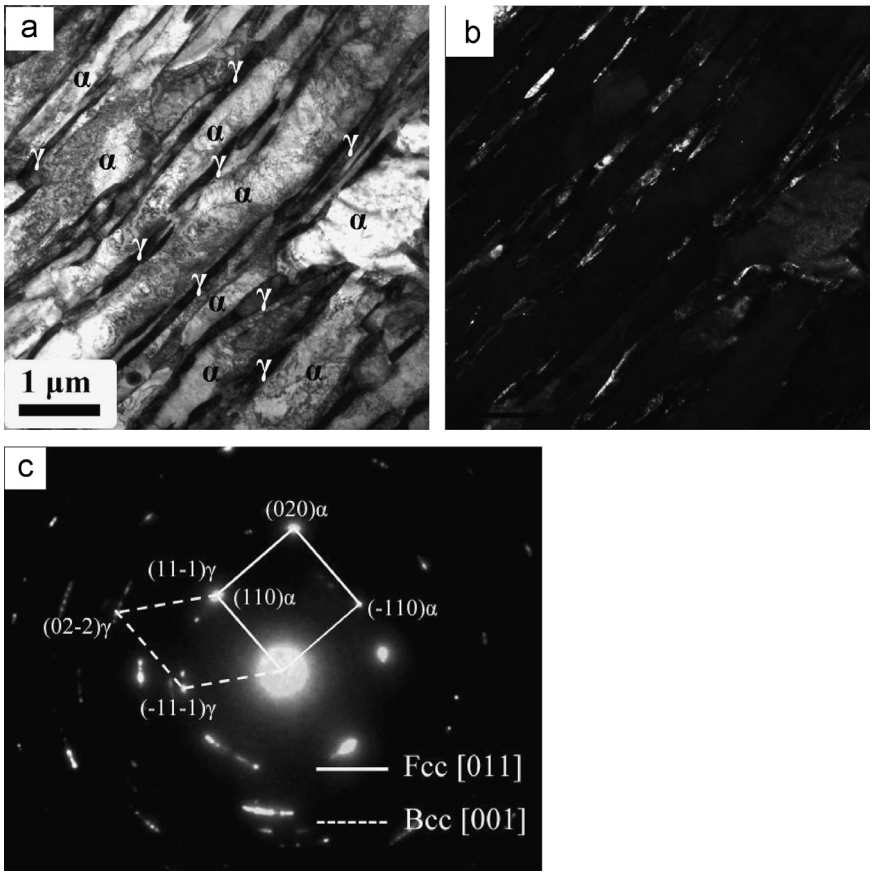

Fig. 6. (a) Bright field, and corresponding (b) dark field micrograph, and (c) selection area diffraction pattern showing lamellar-type retained austenite present between bainitic laths in the steel tempered at 500 °C for 60 min.

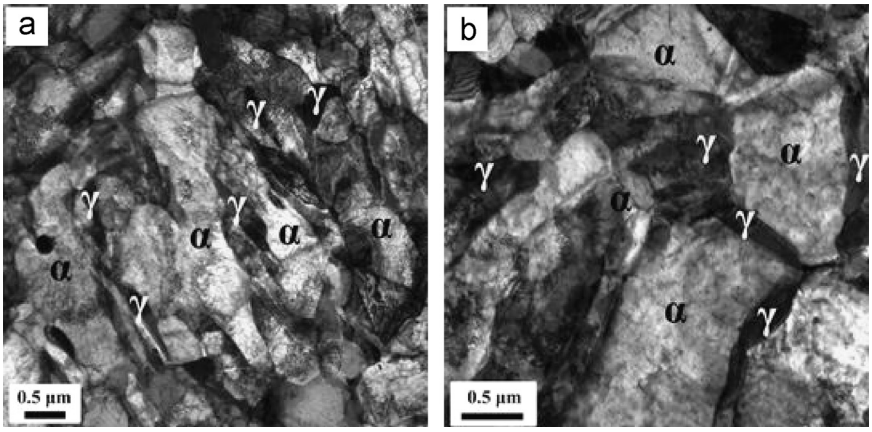

Fig. 7. (a) Low and high magnification bright field micrographs showing the quasi-polygonal ferrite, coarse bainitic/martensitic lath, and retained austenite in the steel tempered at 500 °C for 120 min.

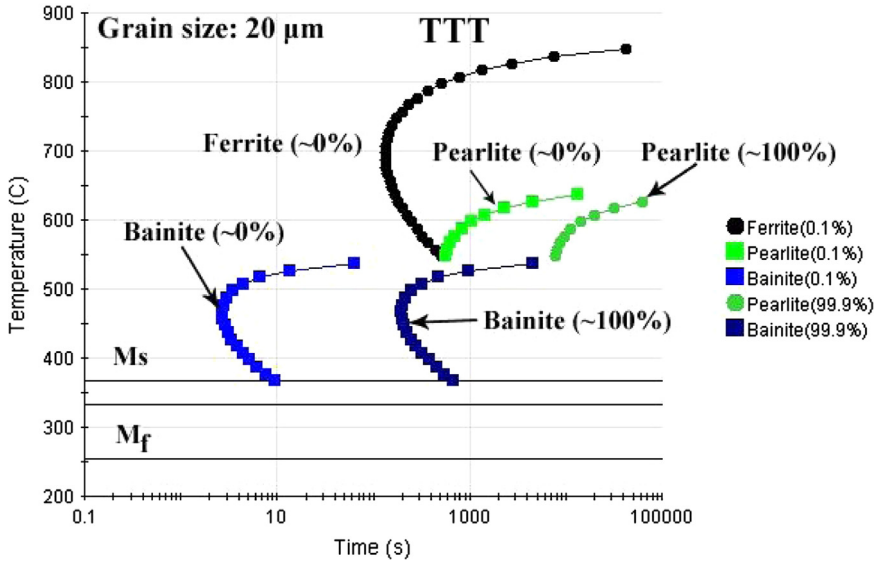

Fig. 8. Time-temperature-transformation diagram of experimental steel as concluded from JMatPro.

the occurrence of reversion transformation at low tempering temperature is minimal. Compared with the volume fraction of retained austenite (~29%) obtained by two-step heat treatment, the results here indicate that the retained austenite has high thermal stability during the tempering process.

Two factors contribute to the high stability of retained austenite. (i) *The chemical composition*: the reversed austenite was enriched with manganese, nickel and copper, which is expected to significantly increase the stability of retained austenite [13,14]. Because of low carbon concentration [5] in retained austenite and high Si and Al content that suppress the formation of cementite, retained austenite hardly decomposes into ferrite and cementite during the tempering process. In addition, it was suggested that retained austenite of lower carbon concentration has higher thermal stability [15]. (ii) *Grain size*: the retained austenite obtained in the third tempering step had an average grain size less than 1 μm (Fig. 3). In a ultrafine grained austenite with the grain size less than 1 μm, a huge chemical driving force is required for the nucleation of martensite within the grain and very effective for suppressing martensitic transformation from fcc to bcc structure [16]. Moreover, such small grain size of retained austenite will lower the martensite start temperature and is favorable in rendering austenite stable at room temperature [17,18]. For this reason, high volume fraction of retained austenite was still obtained after tempering process.

3.4. Precipitation during the tempering process

The Vickers hardness-tempering temperature plot is presented in Fig. 10a. The average Vickers hardness value (VHN) of two-step processed steel was 280 VHN. As the tempering temperature was increased from 400 °C to 550 °C, the hardness remained stable in this range, but was decreased at 600 °C (Fig. 10a). This is attributed to strong recovery and ferrite transformation that significantly increases the ferrite content in the steel. Fig. 10b shows the hardness versus tempering time plot of experimental steel at a constant tempering temperature of 500 °C. With increase in tempering time, the hardness was gradually increased. A maximum value of 305 VHN was attained on tempering for 120 min. This behavior indicates that long tempering time facilitates precipitation.

Because precipitates formed in each step are difficult to differentiate due to the short tempering time that cause marginal change in the size, morphology and distribution of precipitates, no

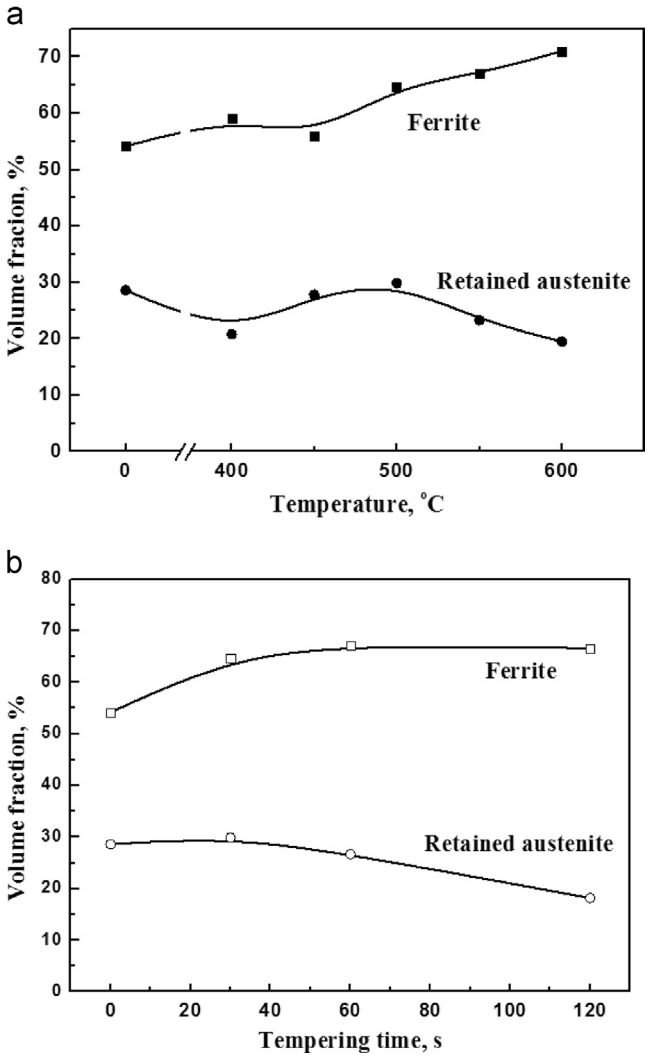

Fig. 9. Effect of (a) tempering temperature at a constant tempering time of 30 min, and (b) tempering time at a constant tempering temperature of 500 °C on the volume fraction of ferrite and retained austenite in the experimental steel. Every data shown in the figure is an average of at least three tests. The measurement errors of volume fraction of ferrite and austenite are below ±1% and ±3%, respectively.

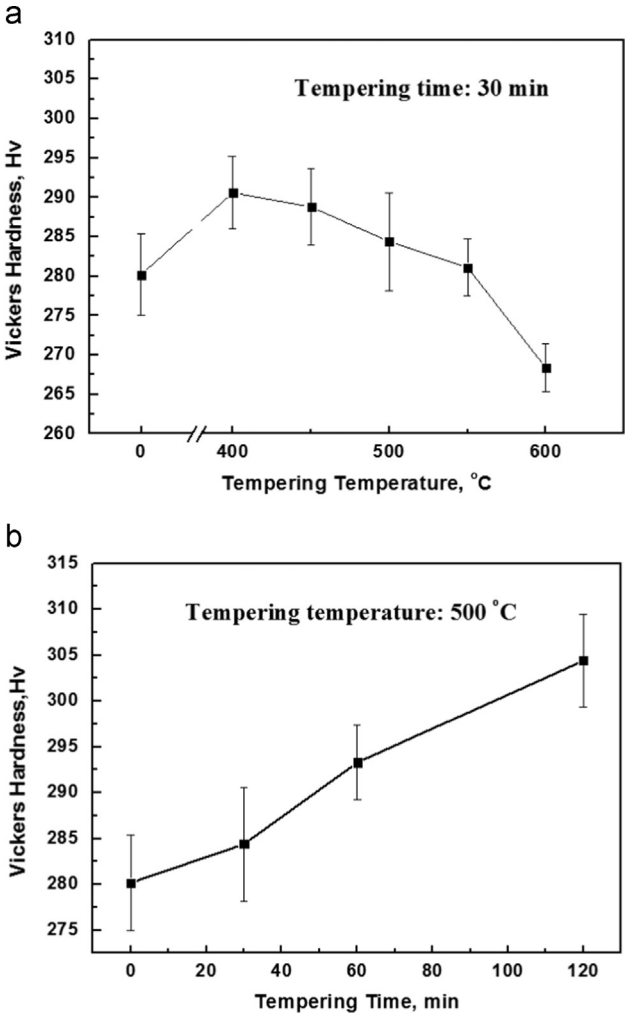

Fig. 10. Vickers hardness as a function of (a) tempering temperature and (b) tempering time in experimental steel processed through three-step heat treatment.

quantitative estimates of precipitation were attempted for the three-step tempered samples. The different precipitates present in the steel due to micro-alloying were analyzed in terms of size, morphology, and precipitation sites using TEM. Two types of precipitates were observed (Figs. 11 and 12). The first type is the precipitates that are oblong and irregular in shape, and distributed in the ferrite matrix. They were identified as NbC precipitates (black dot dash area in Fig. 12b). The second type with larger size is spherical and is distributed in both ferrite and retained austenite (Fig. 11 and white dash area in 12b). EDX analysis of these precipitates confirmed high concentration of copper. The select area diffraction (SAD) pattern indicates the orientation relationship between ferrite and copper precipitates as Kurdjumoch–Sachs (K–S) relationship $[111]_{\alpha}//[110]_{Cu}$. The investigation of copper precipitation in austenitic steel suggested that copper precipitates were formed after the formation of Cu-rich area that was formed by the diffusion of copper during aging stage, such that a long aging time was required [19]. In the present case, the prior two-step intercritical process at high temperature facilitate the enrichment of copper in reversed austenite [20], leading to the formation of Cu-rich area before the third tempering process. Thus, the precipitation of copper occurred in retained austenite during the tempering process.

4. Discussion

The experimental steel processed by two-step heat treatment exhibited outstanding mechanical properties which are attributed to the cooperation of multiphase microstructure, high retained austenite content and nanometer-size precipitates. From the optical and SEM micrographs of the three-step heat-treated steel, there was no obvious change in microstructure except volume fraction of different phases as compared with the two-step processed steel. It seems that the increased ferrite fraction and decreased retained austenite content may lead to decrease in yield strength and ductility. In spite of this, the formation of copper and niobium precipitates in ferrite and retained austenite would compensate the loss in strength through precipitation strengthening effect, such that yield strength remained stable and even higher at low tempering temperatures and long tempering time. Additionally, the volume fraction of retained austenite was maintained above ~20% even after the tempering process, resulting in high ductility of three-step processed steel.

On the other hand, previous study demonstrated that retained austenite absorbs dislocation from the neighboring martensite during deformation process. This behavior of retained austenite

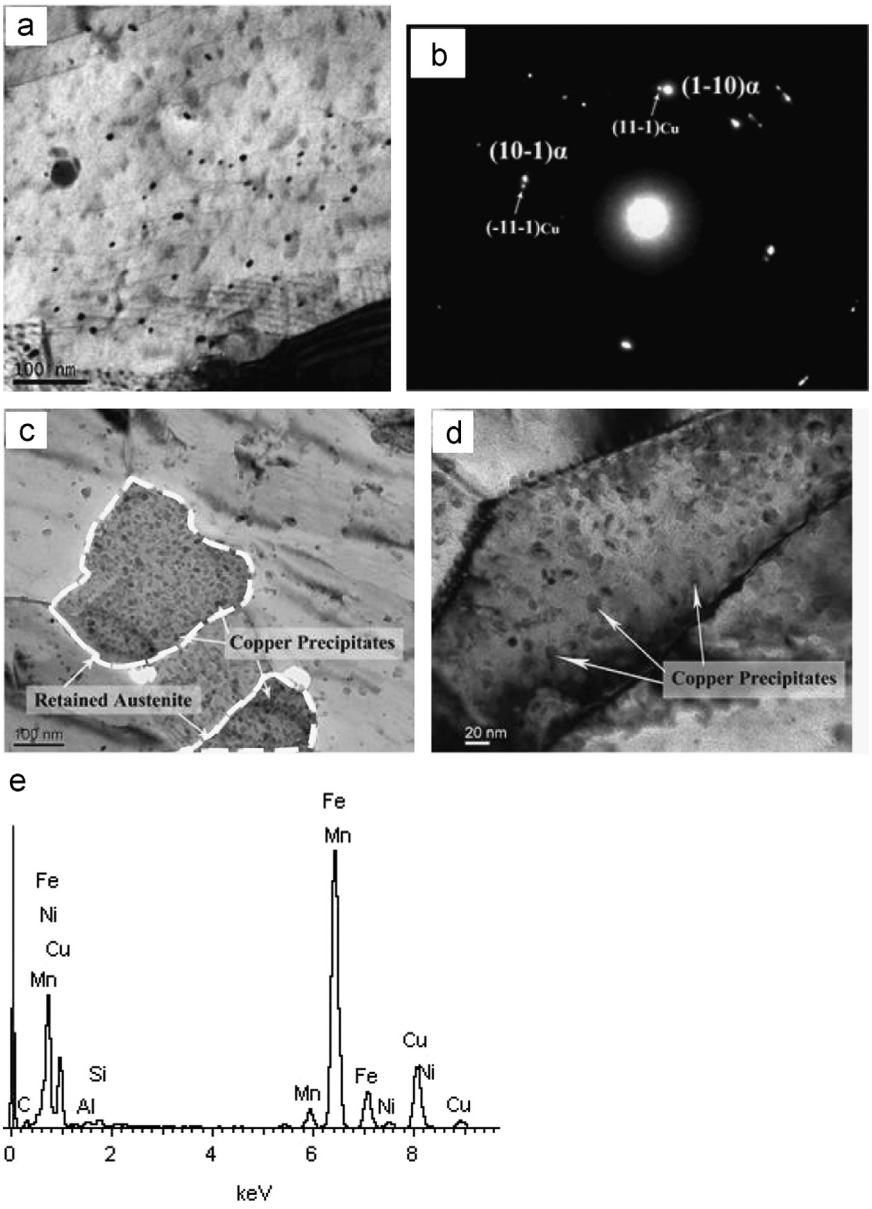

Fig. 11. (a, c, d) Bright field micrographs, (b) selection area diffraction (SAD), and (e) energy dispersive spectra (EDS) showing copper precipitates in ferrite and retained austenite in steel tempered at 500 °C for 30 min.

intensifies the deformation ability of martensite, and is favorable for enhancement of ductility [21]. Copper precipitates in retained austenite are considered to prevent the movement of dislocations, which delay the dislocation accumulation in austenite and slower its transformation to martensite. Second, the precipitates significantly enhanced the strength of retained austenite through hardening effect. Alloy-enriched retained austenite has higher hardness than ferrite [22]. This means that the retained austenite acts as a hard phase in the steel. Since the tensile strength is governed by the volume fraction and strength of the hard phase, the increase in the strength of retained austenite will lead to improvement of tensile strength. Furthermore, the retained austenite transforms to martensite at large strains during the deformation process. The martensite inherits the dislocations and precipitates from the retained austenite. The copper precipitation and high density of dislocation in martensite contribute to enhancement of tensile strength.

From the above discussion, the good combination of strength and elongation observed in the studied steel is a cumulative contribution of retained austenite and co-precipitation of niobium and copper. Precipitation play a dominant role in stabilizing retained austenite during the tempering process, and consequently increases yield and tensile strength.

5. Conclusions

In the present study, a three-step heat treatment was considered to obtain superior mechanical properties in a low carbon microalloyed steel. The present study focused on the impact of third-step tempering process on the structure–mechanical property relationship. In addition, the impact of nanometer-sized precipitates and retained austenite were discussed. The primary conclusions are as follows:

(1) The microstructure of the three-step processed steel comprised of ferrite, retained austenite and tempered bainite/martensite. Ferrite was enriched with niobium-containing and copper precipitates, and ferrite content increased with increase in tempering temperature and time.

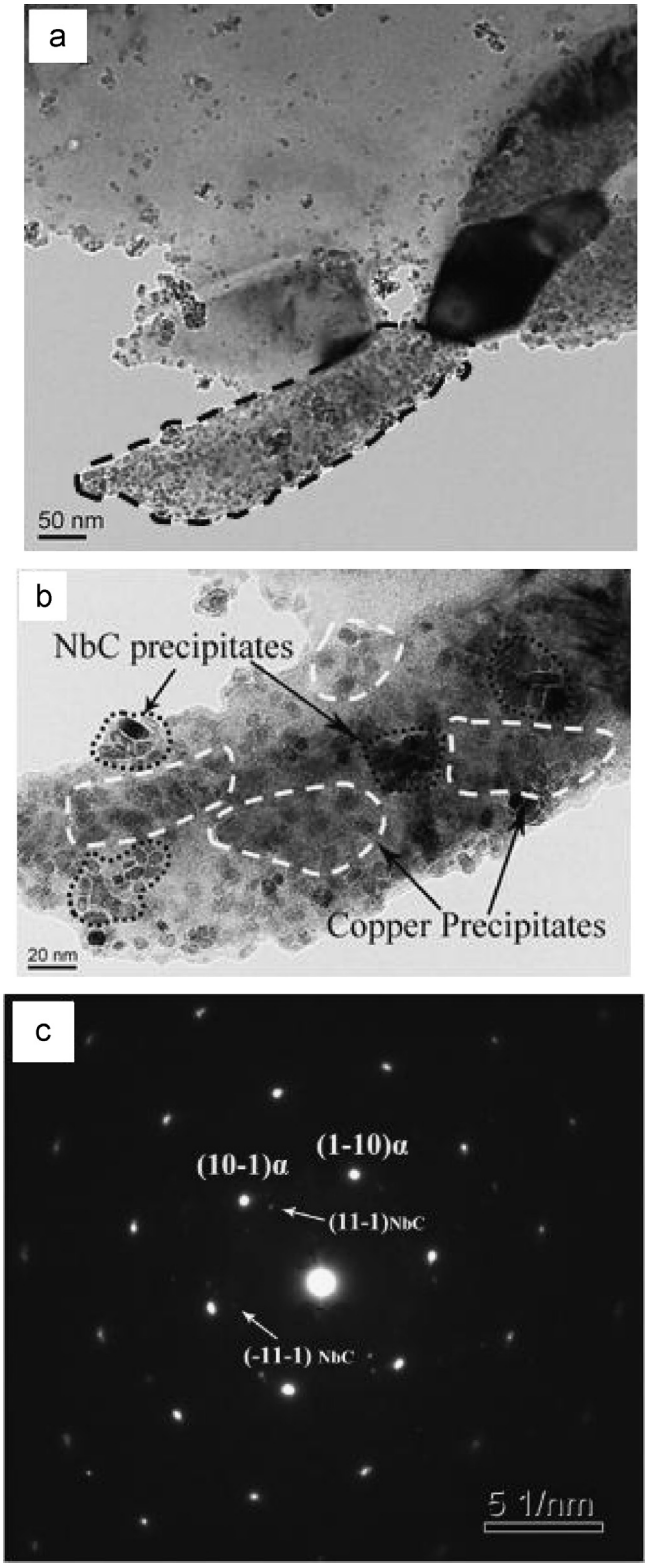

Fig. 12. (a) Low magnification bright field micrographs showing the co-precipitation of copper and niobium in ferrite in steel tempered at 600 °C for 30 min. (b). The high magnification bright field image and (c) diffraction pattern of black dash circle area in (a).

(2) Retained austenite has ultrafine size less than 1 μm, and was enriched with copper precipitates that contribute to enhance the stability of austenite. The volume fraction of retained austenite remained stable between 20% and 30%, showing high thermal stability during the tempering process.
(3) The combination of ultrafine microstructure, retained austenite and nanometer-sized precipitates led to superior mechanical properties: yield strength of 700–750 MPa, and tensile strength of 850–930 MPa, uniform elongation of 20–23%, and total elongation of 30–38%. This is attributed to the cooperation of TRIP effect of retained austenite and precipitation strengthening effect of nanometer-sized precipitates.
(4) The optimal combination of high strength and good ductility was obtained in tempering temperature range of 450–500 °C or by prolonging the tempering time at 500 °C, such that the product of tensile strength and total elongation was greater than 32 GPa%.

Acknowledgment

The authors wish to thank the support from National Basic Research Program of China (973 Program) through contract number 2010CB630801 and the China Scholarship Council for the award of a scholarship to W.H. Zhou to study at the University of Louisiana at Lafayette, USA.

References

[1] R.L. Miller, Metal. Trans. 3 (1972) 905–912.
[2] M. Niikura, J.W. Morris, Metal. Trans. 11 (1980) 1531–1540.
[3] H.N. Han, C.S. Oh, G. Kim, O. Kwon, Mater. Sci. Eng. A 499 (2009) 462–468.
[4] H.W. Luo, J. Shi, C. Wang, W.Q. Cao, X.J. Sun, H. Dong, Acta Mater. 59 (2011) 4002–4014.
[5] W.H. Zhou, H. Guo, Z.J. Xie, X.M. Wang, C.J. Shang, Mater. Sci. Eng. A 587 (2013) 365–371.
[6] W.H. Zhou, X.L. Wang, P.K.C. Venkatsurya, H. Guo, Z.J. Xie, C.J. Shang, R.D. K. Misra, Mater. Sci. Eng. A 607 (2014) 569–577.
[7] G. Thomas, Metal. Trans. A 9A (1978) 439–450.
[8] S. Hashimoto, S. Ikeda, K. Sugimoto, S. Miyake, ISIJ Int. 44 (2004) 1590–1598.
[9] T.Y. Hsu, Z.Y. Xu., Mater. Sci. Forum 561–565 (2007) 2283–2286.
[10] F.S. LePera, Metallography 12 (1979) 263–268.
[11] M.J. Santofimia, T. Nguyen-Minh, L. Zhao, R. Petrov, I. Sabirov, J. Sietsma Mater. Sci. Eng. A 527 (2010) 6429–6439.
[12] M. Farooque, H. Ayub, A. Haq, A.Q. Khan, Mater. Trans. 39 (1998) 995–999.
[13] Z.J. Xie, S.F. Yuan, W.H. Zhou, J.R. Yang, H. Guo, C.J. Shang, Mater. Des. 59 (2014) 193–198.
[14] Z.J. Xie, Y.Q. Ren, W.H. Zhou, J.R. Yang, C.J. Shang, R.D.K. Misra, Mater. Sci. Eng. A 603 (2014) 69–75.
[15] A. Saha Podder, I. Lonardelli, A. Molinari, H.K.D.H. Bhadeshia, Proc. R. Soc. A 467 (2011) 3141–3156.
[16] S. Takaki, K. Fukunaga, J. Syarif, T. Tsuchiyama., Mater. Trans. 45 (2004) 2245–2251.
[17] H.S. Yang, H.K.D.H. Bhadeshia, Scr. Mater. 60 (2009) 493–495.
[18] E. Jimenez-Melero, N.H. Van Dijk, L. Zhao, J. Sietsma, S.E. Offerman, J.P. Wright, S. Van der Zwaag, Scr. Mater. 56 (2007) 421–424.
[19] C.Y. Chi, J.X. Dong, W.Q. Liu, X.S. Xie, Acta Mater. Sin. 46 (2010) 1141–1146.
[20] W.H. Zhou, H. Guo, Z.J. Xie, C.J. Shang, R.D.K. Misra, Mater. Des. 63 (2014) 42–49.
[21] K. Zhang, M.H. Zhang, Z.H. Guo, N.L. Chen, Y.H. Rong, Mater. Sci. Eng. A 528 (2011) 8486–8491.
[22] B.B. He, M.X. Huang, Z.Y. Liang, A.H.W. Ngan, H.W. Luo, J. Shi, W.Q. Cao, H. Dong, Scr. Mater. 69 (2013) 215–218.